Vol. 45 (2002), 1, 21-30
TRIBOLOGY TRANSACTIONS

Effects of Surface Micro-Geometry On the Lift-Off Speed of an EHL Contact©

M.A. MASEN and C. H. VENNER
University of Twente
Faculty of Engineering
NL 7500 AE Enschede, The Netherlands
and
P. M. LUGT and J. H. TRIPP
SKF Engineering and Research Centre B.V.
NL 3430 DT Nieuwegein, The Netherlands

With decreasing speed the film thickness in an EHL contact decreases. Below a certain speed asperity contact will take place and gradually the contact enters the mixed lubrication regime. Vice-versa, with increasing speed beyond a certain speed the film thickness has reached a level where asperity contacts have become so rare that the contact will be in the full film regime.

It seems only logical to expect that the speed at which the first (or last) significant asperity interactions start to take place is influenced by the micro-geometry of the surfaces. In experiments performed on a two-disk rig under conditions of pure rolling, using one very smooth and one rough disk it was indeed observed that the "lift-off" speed defined as the speed above which full film lubrication prevails, differed significantly for surfaces with a different micro-geometry. The test results can be seen as ranking for the surface micro-geometries in terms of their film generating

Presented as a Society of Tribologists and Lubrication Engineers Paper at the STLE/ASME Tribology Conference in San Francisco, CA October 21-24, 2001
Final manuscript approved September 10, 2001
Review led by Steven Danyluk

NOMENCLATURE

A_d	= deformed roughness component amplitude	$[m]$
A_i	= roughness component amplitude	$[m]$
a	= Hertzian contact length in x-direction $a = (3FR/E\prime)^{1/3}(2\kappa IE\pi)^{1/3}$	$[m]$
b	= Hertzian contact length in y-direction $b = a/\kappa$	$[m]$
D	= gap curvature ratio $D = R_x/R_y = \kappa^2 \frac{IK-IE}{IE-\kappa^2 IK}$	
E	= Young's modulus	$[Pa]$
IE	= elliptic integral (second kind)	
$E\prime$	= reduced elasticity modulus	$[Pa]$
G	= dimensionless parameter $G = \alpha E\prime$	
h	= film thickness	$[m]$
h_c	= nominal oil film thickness	$[m]$
F	= contact load	$[N]$
IK	= elliptic integral (first kind)	
L	= Moes materials parameter $L = G(2U)^{1/4}$	
M	= Moes load parameter $M = W(2U)^{-3/4}$	
p_h	= maximum Hertzian pressure $p_h = (3F)/(2\pi ab)$	$[N \cdot m^{-2}]$
r	= wavelength ratio $r = \lambda_x/\lambda_y$	
R_{1x}	= radius small disk in x-direction	$[m]$
R_{1y}	= radius small disk in y-direction	$[m]$
R_{2x}	= radius large disk in x-direction	$[m]$
R_{2y}	= radius large disk in y-direction	$[m]$
R	= reduced radius of curvature $1/R = 1/R_x + 1/R_y$	$[m]$
R_x	= reduced radius of curvature in x-direction $1/R_x = 1/R_{1x} + 1/R_{2x}$	$[m]$
R_y	= reduced radius of curvature in y-direction $1/R_y = 1/R_{1y} + 1/R_{2y}$	$[m]$
R_a	= surface roughness center line average	$[m]$
R_q	= surface roughness root mean square	$[m]$
R_{q_i}	= undeformed surface roughness root mean square	$[m]$
T	= temperature	$[^oC]$
U	= dimensionless speed parameter $U = (\eta_0 \bar{u})/(ER_x)$	
u_1	= small disk surface velocity	$[m \cdot s^{-1}]$
u_2	= large disk surface velocity	$[m \cdot s^{-1}]$
$\bar{u}$	= entrainment velocity $\bar{u} = (u_1 + u_2)/2$	$[m \cdot s^{-1}]$
V	= experimental contact parameter	
W	= dimensionless load parameter $W = F/(ER_x^2)$	
α	= Pressure viscosity index	$[Pa^{-1}]$
ν	= Poisson ratio	
η_0	= viscosity at ambient pressure	$[Pa \cdot s]$
ϕ_c	= contact measure	
κ	= Aspect ratio contact ellipse	
∇	= generalised dimensionless wavelength $\nabla = \sqrt{\frac{2}{3}\pi^3(\frac{\lambda}{a})(\alpha p_h)^{\frac{3}{2}}L^{-2}}$	
Λ	= roughness parameter $\Lambda = h/R_q$	
λ	= roughness component wavelength	$[m]$
λ_x	= wavelength in x-direction	$[m]$
λ_y	= wavelength in y-direction	$[m]$
ω_2	= large disk angular velocity	$[rev/min]$

capability. In this paper the question is addressed if a ranking as observed in the tests can be predicted in advance, using the load conditions and the measured surface micro-geometry as input, without having to resort to full-scale numerical simulations of any sort.

Based on the amplitude reduction formula proposed by Venner et al. (2000), for roughness in contacts under pure rolling a model is constructed that, given the load condition and a measured surface micro-geometry, determines the deformed micro-geometry and subsequently a measure of "probability of contact." For a given contact this measure can be plotted as a function of speed to obtain a theoretical "lift-off" curve. For the different types of surface micro-geometries used in the tests such a curve is compared with the experimental results, showing a promising agreement in ranking.

KEYWORDS

Elasto-Hydrodynamic Lubrication; Surface Roughness Effects

INTRODUCTION

Almost three decades ago Dowson and Higginson (1966) and Hamrock and Dowson (1977) presented formulas for the prediction of the film thickness in EHL line and point contacts. These formulas were based on the results of numerical simulations and are still widely used today. This is not surprising, as comparison with experimentally obtained values, e.g. using optical interferometry, has shown that they are quite accurate for a relatively large range of operating conditions. More recently, similar formulas based on more comprehensive computations have extended the range of conditions for which accurate film thickness predictions are available, e.g. see Nijenbanning et al. (1994). However, these formulas are based on the assumption of perfectly smooth surfaces, and in reality engineering surfaces are never perfectly smooth.

To determine the effects of surface roughness on film formation and performance of an EHL contact, the micro-geometry of the surfaces should somehow be accounted for. Traditionally, the lambda ratio: $\Lambda = h/R_q$ has been used as an indication of the effect of roughness on the lubrication condition of the contact, where h is the film thickness for smooth surfaces, and R_q is taken as the rms deviation of the measured surface from its mean plane. This parameter particularly appears in the presentation of the results obtained with statistical approaches with an averaged model equation. Typical examples are the works of Christensen (1970), Elrod (1979), Patir and Cheng (1978, 1979) and Tripp (1983). For example, it is assumed that the transition from mixed to full film is reached for $\Lambda > 3$.

Although widely used in practice, the value of criteria based on the lambda ratio is questioned for several reasons, see Venner et al. (1991, 1992) and Cann et al. (1994). Firstly, the Λ ratio is generally computed using for R_q the value for the *undeformed* surface. For hydrodynamic lubrication problems in journal bearings this is justified, but in EHL contacts the deformation of the micro-geometry may be considerable, and moreover will depend on the sliding conditions. However, even if R_q were calculated for the deformed roughness, it is still questionable if such a single *global* parameter can discriminate adequately the performance of surfaces with different surface topography. For one thing, the shape and not just the height of a surface feature determines the hydrodynamic pressure it can generate.

An alternative to these statistical approaches is the deterministic approach where the problem is solved using a detailed description of the surface including its micro-geometry. A prerequisite for such studies is a fast and stable algorithm for the numerical solution of the governing equations. In the past decade the capability to numerically simulate EHL contacts has seen an enormous advance. Owing to efficient and stable algorithms, e.g. based on multigrid/multilevel techniques (Venner et al. (2000)), presently transient simulations with large numbers of grid points are feasible. As a result of the algorithm improvement, gradually more complex problems were studied including the (steady and transient) effects of single features like waviness and dents and ridges, see e.g. Venner (1991), Ai et al. (1994), Chang et al. (1989), Goglia et al., (1984), Kweh et al. (1989), Lubrecht et al. (1988), Venner et al. (1991), (1994), (1996). The advantage of application to such well-defined features is that the accuracy of the simulations can be verified easily. Also, using optical interferometry techniques as described in Kaneta et al. (1992) and Wedeven et al. (1979), experimental validation can be obtained for the results (Venner et al. (1994), (2000)). Moreover, with the advanced version of this technique using a spacer layer, one can even measure for very thin films (Cann et al. (1996) and Guangteng et al. (2000).

The use of numerical simulations to study the effects of real measured roughness profiles seems a logical next step, (Venner et al. (1992), Ai et al. (1994), (1996), Chang et al. (1991), Xu et al. (1996) and even extensions of the usual Reynolds based models to "mixed" models allowing asperity contacts to occur have recently been reported (Hu et al. (2000) and Redlich et al. (2000)). However, the step from singular features to real roughness, even for the fully flooded case, should not be taken lightly. Firstly, the accuracy of the results is hard to verify whereas it is of the utmost importance to show that trends observed in the solutions are indeed rooted in the physcico-mathematical model, rather than strongly influenced by, or even artefacts caused by the numerical process (among which the discretisation error). Even setting these problems aside, numerical simulations for real rough surfaces will generate an enormous amount of data from which it is difficult to extract trends or criteria to be used in design or surface optimisation. Finally, even with today's generation of fast solvers and computer hardware, full-scale transient numerical simulations on dense grids are time-consuming. It would be of great help if, for a crude optimisation, a simple predictive tool were available that enables evaluation of different roughness patterns with respect to their effect on e.g. the film thickness. This applies in particular if the aim is to "design" an optimal micro-geometry. The simple tool could then be used to quickly evaluate a large number of candidate surfaces.

These considerations have led to the approach introduced in (Venner et al. (1997)). Instead of solving the real rough surface problem, the deformation of harmonic patterns (waviness) has been determined in detail. First the line contact problem was stud-

TABLE 1—TWO-DISK RIG TEST CONDITIONS AND PARAMETERS CHARACTERIZING THE CONTACT	
R_{1x}	10 *mm*
R_{1y}	∞ (flat)
R_{2x}	50 *mm*
R_{2y}	50 *mm*
ω_2	40 - 1600 *rev/min*
$u_1 = u_2 = \omega_2 R_{2x}$	0.21 - 8.4 *m/s*
E	$2.06\ 10^{11}$ *Pa*
ν	0.3
T	40°*C*
η_0	$7.681\ 10^{-3}$ *Pa•s*
α	$1.67\ 10^{-8}$ Pa^{-1}
F	1000 *N*
E'	$2.26\ 10^{11}$ *Pa*
HERTZIAN DRY CONTACT PARAMETERS	
a	$0.273\ 10^{-3}$ *m*
b	$0.885\ 10^{-3}$ *m*
κ	0.309
p_h	$1.97\ 10^{9}$ *Pa*
DIMENSIONLESS EHL PARAMETERS	
M	$4.26\ 10^{4}$ - $2.68\ 10^{3}$
L	4.3 - 10.9
G	3780
U	$8.5\ 10^{-13}$ - $3.4\ 10^{-11}$
W	$6.4\ 10^{-5}$

ied (Venner et al. (1997)). It was shown that the reduced relative amplitude under pure rolling could be predicted accurately with a function of a single non-dimensional parameter. Theoretical support for this behaviour was provided by Hooke (1997). Next it was shown that the amplitude reduction of harmonic patterns in a circular contact followed the same behaviour (Hooke et al. (1999), (2000) and Venner et al. (1999)), and the work was extended to elliptic contacts in Venner et al. (2000). These results show that there appears to be a unifying mechanism governing the amplitude reduction of harmonic patterns in EHL contacts. The potential of this work for practical purposes is large. Assuming linear independence of the roughness components, an estimate of the deformed roughness inside the contact can be obtained by decomposing the micro-geometry into its Fourier components, using the amplitude reduction curve as a filter giving the deformed amplitude of each component followed by an inverse Fourier transform to assemble the output in the form of the deformed profile. Hence, to obtain this estimate of the deformed profile no numerical elastohydrodynamic simulations for real roughness will be needed and the resulting tool can be used in an engineering environment.

The focus of the present work is to investigate if this "amplitude reduction" model can be used to predict the effects of surface micro-geometry on the film generating capacity of a contact. For this purpose experiments have been performed on a two-disk machine, using capacitance measurements to monitor the lubrication condition of the contact as a function of the velocity of the surfaces in contact. Tests have been performed with one very smooth surface and an opposing rough surface with varying roughness both in magnitude as well as in topography. These tests

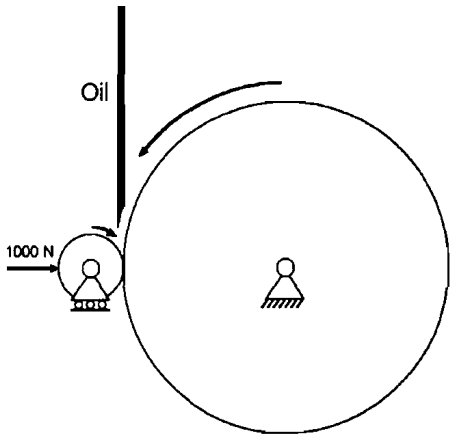

Fig. 1—Schematic representation of the two-disk test rig.

provide a ranking of the surfaces in terms of the speed at which full film lubrication is achieved. It is investigated to what extend this ranking is also found with the developed simple model.

EXPERIMENTAL SET-UP

Figure 1 shows the basic configuration of the two-disk rig used for the experiments. A small and a large disk, simulating the contraform contact between roller and inner ring of a bearing, run against each other under *fully flooded pure rolling* conditions. The contacting surface of the small disk is cylindrical, but to avoid misalignment problems the large disk is crowned. A situation of "single sided" roughness was created by manufacturing the large disk to very low roughness values and using small disks with surfaces with different micro-geometries. The micro-geometry was varied both in terms of its magnitude as well as its morphology. Also the experiments were performed under pure rolling conditions and the supply of oil was sufficiently large to ensure a fully flooded contact. These measures were taken to maximise the reproducibility of the test conditions, thus reducing the likelihood that results might be influenced by other effects, such as variations in thermal or starvation conditions. Table 1 gives the details of conditions.

LIFT-OFF

In the experiments, for a given load the speed is stepwise increased from zero to 1600 rev/min. The lubrication condition of the contact is monitored using a capacitance/resistance measurement technique, as described in Heemskerk et al. (1982). The technique is operated in a mode with a high frequency alternating current of 410 kHz. This is preferred to DC and low frequency AC techniques (i.e. resistance measurement) because these latter modes may lead to the formation of polarised layers on the surfaces. For each speed step, the signal is averaged over time and the time-average signal at zero speed is adjusted to zero. The resulting curve of the capacitance signal *vs.* speed is referred to as the *lift-off curve*.

At this point it should be noted that at lower speeds, changes in the EHL film thickness result in changes in the average fraction of surface in contact, so that here the lift-off curve measures the resistive impedance of the contact and actually maps the Abbott-

TABLE 2—ROUGHNESS OF THE TWO-DISK RIG SAMPLES

SURFACE FINISH	R_a (μm)	R_q (μm)
Ground, very smooth	0.08	0.10
Ground, smooth	0.14	0.18
Ground, rough	0.22	0.28
Ground, very rough	0.24	0.31
Stone honed	0.07	0.10
Cross honed	0.09	0.12
Isotropic	0.10	0.13
Ground	0.08	0.11

Firestone or cumulative bearing area curve of the deformed roughness height distribution. At higher speeds, where very little metallic contact survives, the impedance measures the capacitance across the oil film and the slope is determined directly by the increase of EHL film thickness with speed. Hence, compared to the resistance-dominated end, the slope of the lift-off curve becomes very small.

The lift-off curve may be normalised using its value at 1600 rev/min where there are essentially no metal-to-metal asperity contacts and the contact as a whole operates in the full film regime. From the *normalised lift-off curve* the transition from the mixed to the full film regime can now be said to occur at the speed where the normalised lift-off signal reaches a given value, i.e. 0.9. At zero speed no hydrodynamic pressure is generated so that the pressure distribution then is the same as in dry rough contact, corresponding to a real contact area fraction of approximately one half. For a contact operating at the lift-off speed, then, about 90% of this half is lifted off. Assuming an approximately linear relation between the lift-off signal and real contact area this would imply that the mixed lubrication regime is defined to end when less than 5% metallic contact exists.

TEST PROCEDURE

Each experiment is started with a low load warm-up sequence of about one hour at 1000 rev/min. Subsequently, the load is increased to the target load of 1000 N and the speed ramped up and down again in five consecutive speed-sweeps. During the first three speed-sweeps the lift-off signal gradually develops to a steady-state lift-off curve. This is caused by the removal of the boundary layers on the surfaces. To minimise any of these effects, only the results from the final speed sweep were taken. Samples of the various surfaces were measured both before and after the lift-off experiments using an interferometric optical profiler. No significant changes in surface geometry were observed.

EXPERIMENTAL RESULTS

The large disk was polished to a very low roughness: $R_a \approx 0.015\ \mu m$. Small disks were used with different microgeometries, see Table 2. The parameters R_a and R_q for the undeformed roughnesses of the different small disks are given in the table. To facilitate comparison of the results it is convenient to distinguish two groups. The first group is characterised by the fact that the surface preparation method is the same (grinding), but the magnitude or amplitude of the roughness is different. As can be

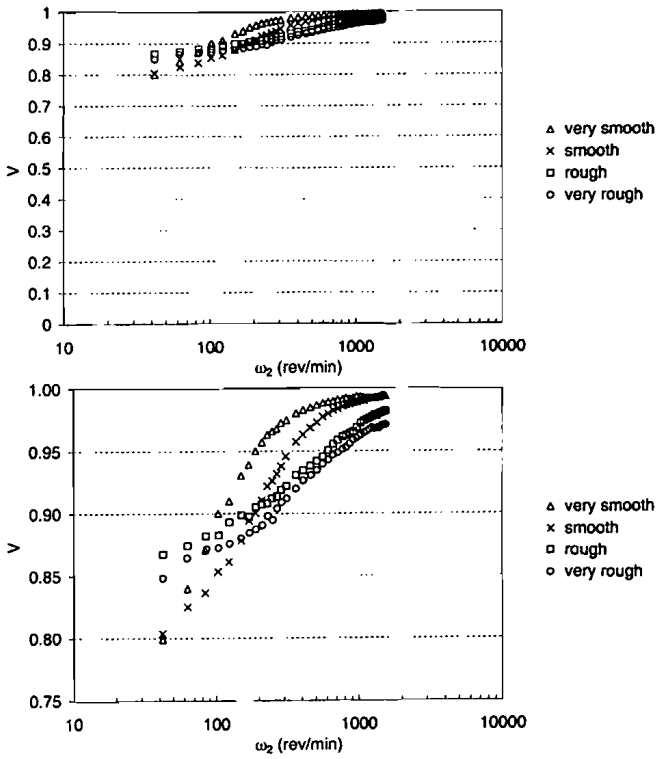

Fig. 2—Measured lift-off curves for ground surfaces with different roughness. Surface roughness parameters can be found in Table 2.

seen from Table 2 they cover a relatively large range of R_a values. The second group consists of surfaces manufactured by different processes. The separation into two groups was done to isolate so far as possible the effect of "amplitude" of the roughness from other effects of morphology.

GROUND SURFACES

Figure 2(a) shows the lift-off curves measured for the ground surfaces: the relative voltage signal V as a function of the speed. All curves show the same typical behaviour. With increasing speed the signal increases indicating an increasing film thickness and decreasing amount of asperity contacts until at high speed the contact is fully lubricated. At first sight the curves for the different surfaces seem to differ little. However, approaching the high speed end of the curve a clear separation emerges which shows that the speed at which the contact achieves particular percentage of the maximum signal differs significantly for the different surfaces. This is more clearly visible in the enlargement shown in Fig. 2(b). Defining the lift-off speed as the value of the speed when the signal has reached 90% of its maximum value, this lift-off speed is larger for a rougher surface (larger R_a). This indicates that with increasing roughness amplitude the transition from mixed lubrication to hydrodynamic lubrication takes place at a larger value of the nominal film thickness as is consistent with common expectations. In terms of "film generating" performance this also implies that the surfaces rank according to their R_a value: "good performance" and lift-off at low speed for the very smooth ground surface, and "bad performance" implying lift-off at a higher speed for the very rough ground surface. However, this "logical ranking" only applies to the high speed end of the curve,

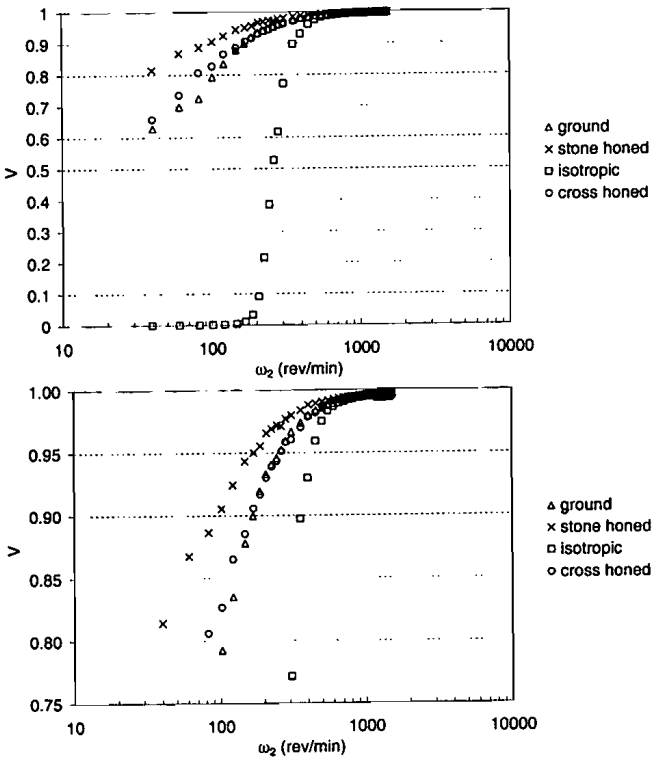

Fig. 3—Measured lift-off curves for processed surfaces with different topography. Surface roughness parameters can be found in Table 2.

which can be interpreted as the region in which full film behaviour dominates and the amount of asperity contacts is relatively small. If the lift-off speed were defined at a value of V significantly lower than 90% the ranking would be different. This possibly indicates that different mechanisms influence the transitions from full contact to mixed lubrication and from full film to mixed lubrication. The theoretical model to be described later is aimed at the transition from the full film to the mixed lubrication regime, i.e. when the total amount of asperity contacts is small. This is why the lift-off speed was defined at a high value of V. It is the purpose to predict the ranking in this high speed end of the curve correctly.

PROCESSED SURFACES

The test results for the group of processed surfaces characterised by the fact that they have a micro-geometry with a different topography are presented in Fig. 3(a). The figure clearly shows that the surface topography affects the lift-off behaviour. Again defining the lift-off speed as the value at which the signal has reached 90% of its maximum value it now appears that the isotropic surface has the highest lift-off speed and thus the worst performance. The cross honed surface has a performance comparable to the basic ground surface, and the stone honed surface shows the best performance. This is shown even more clearly in Fig. 3(b).

THEORETICAL MODEL

The aim of the theoretical study is to find out if the ranking exhibited by the experimental results can be predicted using a simple theoretical model. This model consists of two steps. In the first step the deformed micro-geometry is determined using the "amplitude reduction" formula of Venner and Lubrecht. In the second step, combining the deformed micro-geometry with a nominal film thickness, an estimate of a probability of contact is computed.

DEFORMED MICRO-GEOMETRY

For harmonic surface patterns the amplitude of film thickness oscillations inside the contact as a function of the initial amplitude, the wavelength and the load conditions, under pure rolling conditions was studied in Venner et al. (1997), (1999), (2000). The waviness causes a *film thickness oscillation* inside the contact with a constant amplitude A_d around a nominal film thickness that roughly equals the film thickness for smooth surfaces. The wavelength of this oscillation equals the wavelength of the undeformed pattern. It was found that the ratio of A_d to the undeformed amplitude of the *waviness* A_i was a function of a single non-dimensional parameter ∇ defined as:

$$\nabla = \sqrt{\tfrac{2}{3}}\pi^3(\tfrac{\lambda}{a})(\alpha p_h)^{\frac{3}{2}}L^{-2} \qquad [1]$$

where λ is "the wavelength" of the pattern, α the pressure viscosity index of the oil, p_h the maximum Hertzian pressure, and L the Moes materials parameter. Hence ∇ can be seen as a generalised wavelength. In terms of this generalised wavelength it was found that high frequency waviness (small ∇) results in oscillations with an amplitude $A_d \approx A_i$ whereas low frequency waviness results in oscillations with a very small amplitude $A_d/A_i \approx 0$. For an harmonic pattern with wavelength λ_x in the direction of the flow and λ_y in the transverse direction it was found that the relative amplitude of the film thickness oscillation inside the contact is quite accurately predicted by the formula:

$$\frac{A_d}{A_i} = \frac{1}{1+0.15\bar{f}(r)\nabla+0.015(\bar{f}(r)\nabla)^2} \qquad [2]$$

where $\bar{f}(r) = \begin{cases} e^{1-\frac{1}{r}} & \text{if } r > 1 \\ 1 \text{ otherwise} \end{cases}$

with $r = \lambda_x/\lambda_y$

Figure 4 shows A_d/A_i as a function of the generalised wavelength ∇ according to Eq. [2]. The figure reflects that the amplitude of the oscillations inside the contact equals the undeformed amplitude for small ∇ and reduces with increasing ∇.

Although strictly A_d denotes the amplitude of the *film thickness oscillations*, as the nominal film thickness inside the contact is roughly constant and the amplitude of its oscillations varies little over the contact width, it can be taken as a good approximation of the amplitude of the *deformed waviness*. Equation [2] then states that low frequency components (long wavelengths, $\nabla \to \infty$) are flattened completely, whereas high frequency components (short wavelengths, $\nabla \approx 0$) hardly deform at all. This wavelength-dependence of the reduced amplitude is illustrated in Fig. 5. In this figure the undeformed and deformed waviness is given for a sinusoidal wave with a long (a), a medium (b) and (c) a short wavelength.

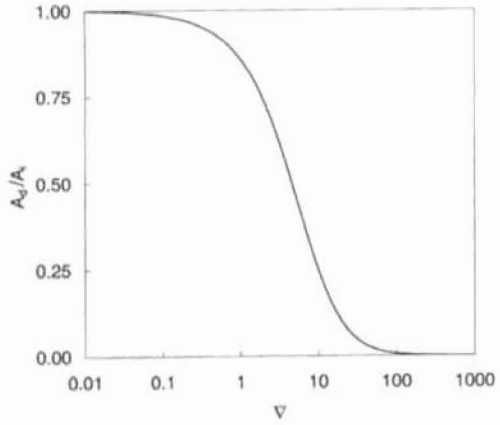

Fig. 4—Generalised "amplitude reduction" curve.

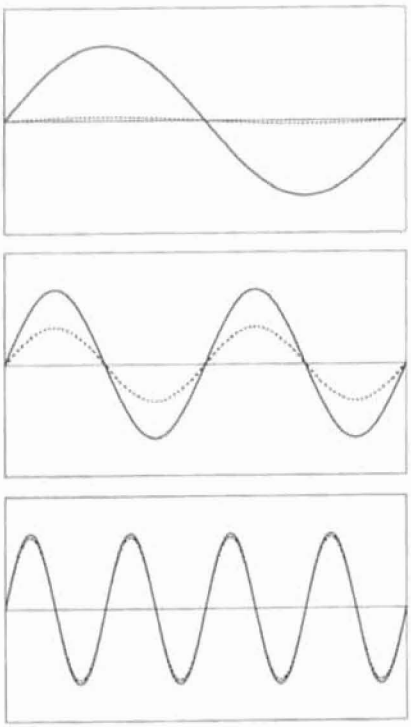

Fig. 5—Undeformed and deformed profiles for sinusoidal patterns of different wavelengths.

At this point it is important to note that for a roughness with a particular wavelength λ the value of ∇ depends on the operating conditions. The terms "short wavelength" and "long wavelength" thus have a relative meaning. Any wavelength is fully deformed at low speed but becomes steadily less deformed as the speed increases, i.e. moving from right to left along the curve in Fig. 4.

The amplitude reduction formula (Eq. [2]) may now be used to predict the deformed surface inside a contact for a general (measured) rough surface profile, following the 3-step procedure:

- Fast Fourier Transform to decompose the surface profile into its individual harmonic components.
- Determination of the reduced amplitude of each of the harmonics using Eq. [2].

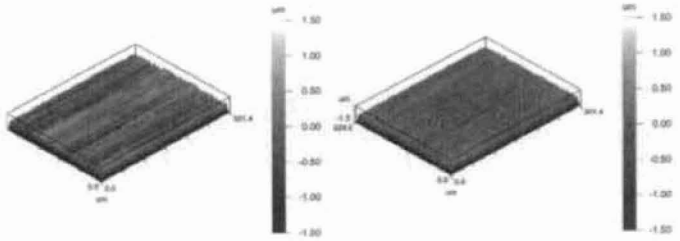

Fig. 6—Undeformed (measured) surface micro-geometry (left) and deformed micro-geometry computed using the theoretical model (black).

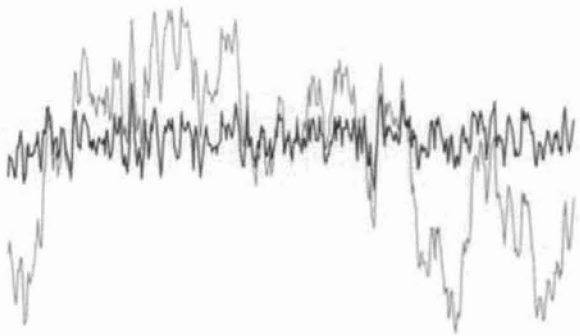

Fig. 7—Undeformed (measured) surface micro-geometry (grey) and deformed micro-geometry computed using the theoretical model (black).

- Inverse Fast Fourier Transform to combine the individual deformed harmonic components into the deformed surface profile.

As an example Figs. 6 and 7 show maps of the undeformed surface micro-geometry of a ground surface and a typical cross-section. The grinding pattern can clearly be recognised. On top of this grinding pattern appears a more high frequency roughness. The figures also show the map and cross-section of the computed deformed micro-geometry under certain load and speed conditions. Comparing the deformed and the undeformed profile shows that whereas the highest frequencies remain present, the lower frequencies have deformed and are pushed away. This is exactly as one would expect based on the Amplitude Reduction curve.

CONTACT MEASURE

Using a given undeformed micro-geometry, the model as described above allows the computation of a deformed micro-geometry. Subsequently from this deformed micro-geometry one can compute a contact measure ϕ_c. This measure is defined as the Abbot-Firestone bearing area ratio of the deformed surface at height h_c, with h_c calculated using a standard smooth film thickness formula Eq. [3]. Its value determines the gap between the smooth counter-surface and the mean plane of the rough surface. At zero speed the nominal film thickness is zero, resulting in a probability of contact of about 0.5 in agreement with independent experimental observations. The "calculated lift-off signal" is now taken as $(1 - (2 \cdot \phi_c))$.

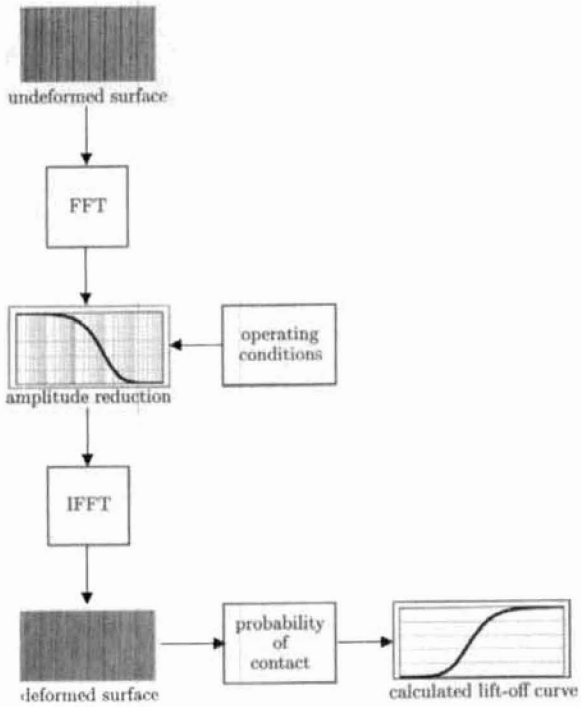

Fig. 8—Overview diagram of the theoretical model.

MODEL SUMMARY

The complete model is summarised in Fig. 8. As mentioned above, it is a very simple model aimed at engineering practice and many simplifications are made. For example by using a smooth film thickness formula for h_c and simply introducing the deformed roughness profile into this gap to find the level of metallic contact, any detailed effects of asperities or asperity contact on the lubricant flow and its pressure generation are ignored.

MODEL ANALYSIS

To understand semi-quantitatively the numerical behaviour of the deformed roughness lift-off model, a simplified analysis may be carried out assuming Gaussian Roughness, a height distribution resulting from many different machining processes.

Experimentally, the measured lift-off curves show contact potential difference against speed and it is assumed only that this potential decreases monotonically as the degree of asperity contact, ϕ_c, increases. In fact, taking the exponent of the speed U in the film thickness formula as approximately 2/3, the abscissa measures the film thickness h to the power 3/2, which is taken as the gap between the mean planes of the two surfaces.

Rigid Roughness

For rigid roughness the calculated lift-off curve is expected to resemble the cumulative height distribution of the roughness, i.e. the Abbott-Firestone bearing area curve, stretched out at the high speed end due to the mapping of h on $h^{3/2}$. A Gaussian distribution gives more-or-less the characteristic shape of the lift-off curve. If the authors take the lift-off speed as the speed at which 5% of the surface exceeds h, this corresponds to a film thickness of about $1.64 \cdot R_q$, i.e. $\Lambda = h/R_q = 1.64$. The authors take this value as determining lift-off. Since R_q is constant, Λ is proportional to h and increases monotonically with the abscissa.

Deformed Roughness

This simple picture changes significantly when the roughness becomes deformed by its passage through the loaded contact. Denoting by R_{q_i} the undeformed roughness, the amplitude reduction curve given by Eq. [2] or Fig. 4 actually shows R_q/R_{q_i} as ordinate, if the spectrum of the surface is approximated by a single frequency or a narrow band of frequencies. Since ∇ contains L, Eq. [2] can be written directly as a function of the dimensionless speed U:

$$R_q/R_{q_i} = \left[1 + AU^{-1/2} + BU^{-1}\right]^{-1} \qquad [3]$$

where A and B contain the characteristic wavelength of the roughness. For the present considerations, the simple Dowson-Hamrock film thickness formula may be adopted:

$$h/R_{q_i} = (C/R_{q_i})\, U^{0.67} \qquad [4]$$

A, B and C all depend on the operating conditions of the contact and may be evaluated from the data in Table 1. Dividing Eq. [4] by Eq. [3] yields an expression for Λ of the deformed roughness as a function of U:

$$\Lambda = h/R_q = (C/R_{q_i})\, U^{0.67}[1 + AU^{-1/2} + BU^{-1}] \qquad [5]$$

By contrast to rigid roughness, Λ is clearly no longer a monotonically increasing function of U. In fact, $\Lambda \to \infty$ for both $U \to 0$ and $U \to \infty$, in between, it passes through a minimum value. This means that as the speed increases from zero, the degree of contact which starts at zero at first increases and the contact approaches the mixed lubrication regime. After the minimum Λ is reached, of course, the degree of contact decreases again and at high speeds, the contact ends up in the full lubrication regime. Whether it ever enters the mixed lubrication regime must depend on the minimum Λ, which is thus of interest to calculate.

From the form of Eq. [2], constants A and B are related by $B^{1/2} = 0.8165A$ and for this case, the minimum of Λ occurs at $U = 0.32B$ with the value $\Lambda_{min} = 2.93\,(CB^{0.67}/R_{q_i})$. Taking all the required values from Table 1 and assuming $r = 1$ yields the following results:

$$\begin{aligned} A &= 6.37 \cdot 10^{-6}\,(\lambda/a) \\ B &= 2.70 \cdot 10^{-11}\,(\lambda/a)^2 = (0.8165A)^2 \\ C &= 3.18 \end{aligned}$$

Figure 9 shows the calculated Λ for surfaces with $R_{qi} = 0.2\mu m$ and with a single frequency or a band of narrow frequencies. Here again the two disk machine configuration (Table 1) is used. $\Lambda_{critical}$, the value of Λ where lift-off occurs is marked in this figure. As stated above, for a Gaussian surface $\Lambda_{critical} = 1.64$.

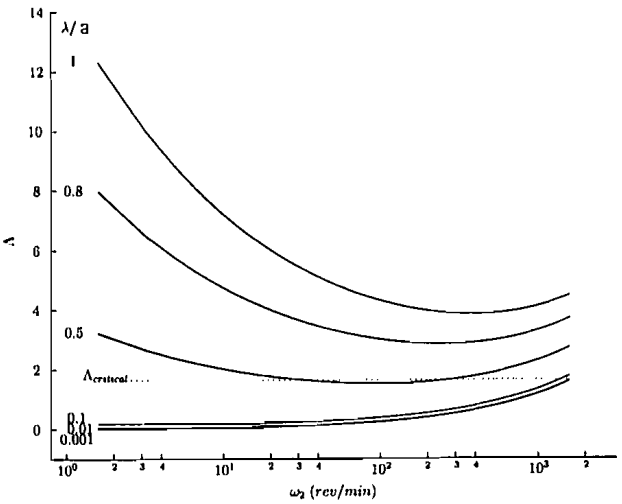

Fig. 9—Calculated Λ for surfaces with a band of narrow frequencies.

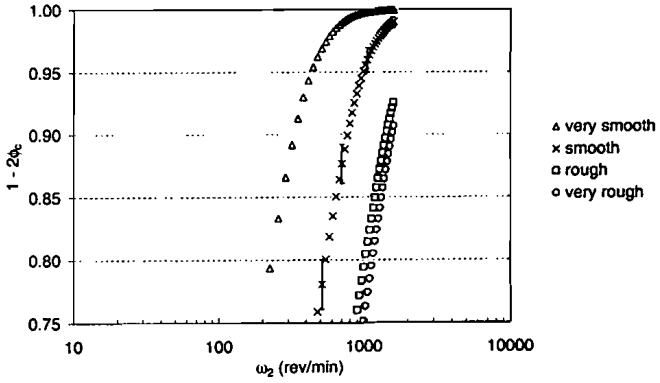

Fig. 10—Theoretical lift-off curve for the ground surfaces. Surface roughness parameters can be found in Table 2.

This figure reveals much about the nature of the deformation of the roughness. For surfaces with a relatively short wavelength (λ/a small), which at any given speed is less deformed, Λ_{min} occurs at an extremely low speed and has a low value, putting the contact well within the mixed lubrication regime. Because the minimum angular speed of the used two-disk rig is about $40\ rev/min$, the part of the lift-off curve at speeds lower than that at which Λ_{min} occurs is not observable for surfaces with such low frequencies. As a result the whole measurable part of the curve lies in a region where Λ increases with speed, starting from a value for which the contact operates in the mixed lubrication regime.

In the case of longer wavelengths, however, the roughness is so easily squashed at low speeds that no metallic contact occurs. Even as the speed rises and the roughness is less squashed, the growth of the (smooth) film thickness itself prevents Λ from ever falling to low values (e.g. 1.64) so that, under the assumed operating conditions, such roughness never operates in the mixed lubrication regime. The normalised lift-off curve in this case would start at unity, pass through a minimum at the speed where Λ_{min} occurs, somewhere in the middle of the speed range, and then rise again asymptotically to unity at the top of the speed range. If Λ_{min} is less than $\Lambda_{critical}$ there will be two speeds at which the degree of contact becomes just 5%, i.e. two lift-off speeds, according to the definition. Such a contact would operate best at speeds either below or above the intermediate range of speeds delimited by these two values. Figure 9 shows that such two lift-off speeds can only be found for surfaces with specific wavelengths in the order of a quarter of the Hertzian contact width.

If Λ_{min} is greater than $\Lambda_{critical}$, the wavelength is sufficiently long to ensure that the contact is always in the full film regime, i.e. is permanently lifted off.

For lower frequencies it appears from Eq. [5] that the wavelength of the roughness may have a more dramatic effect on surface contact and the lift-off curve than the traditional $R_{q_i} = R_q$ parameter. Decreasing R_q by a factor of 10 increases Λ_{min} by the same factor, whereas decreasing the wave-number $\equiv \lambda^{-1}$ (i.e. increasing λ) by a factor of 10 increases Λ_{min} by a factor of more than 20. This suggests that the ranking of surface topographies by their lift-off speed should be influenced quite strongly by λ, as well as by R_q. Designing surface roughness can now be directly linked to the application. After all the optimum frequency depends on the operating load, since λ/a is the determining dimensionless parameter. On the other hand, a varies relatively slowly with load, only as the 1/3 power.

THEORETICAL RESULTS

Immediately after the experiments, the surface micro-geometry of the tested rough disk is measured using an optical profiler. This surface roughness data is used as input for the model. As the measured lift-off curves represent the data of the last speed-sweep, this measured data is the closest to the actual micro-geometry associated with the test conditions and all running in that has taken place in the load warm-up process is excluded. To yield an estimate of variations in predictions due to roughness sampling, the surface topography for each small disk was measured at three "characteristic" spots, allowing three theoretical lift-off curves to be computed for each disk.

Figure 10 shows these computed "lift-off" curves for the ground surfaces. The error bars shown in the curve for the smooth ground surface show that the distinction in curves for the various surfaces is significant. The figure shows that the theoretical curves exhibit the same ranking as was found in the experimental tests, according to the (undeformed) R_a or R_q. Clearly this ranking is only to be expected for geometrically similar surface topographies. Thus, in this simplest case at least, the theoretical model does not lead to any unphysical results.

Figure 11 shows the computed "lift-off" curves for the processed surfaces. Also for these surfaces a clear distinction between the curves of the various surface topographies is found. The calculated ranking agrees with the ranking as observed in the experiments. However, the ranking also agrees with the ranking in R_q. As discussed in the section on "Model Analysis," the surfaces used in this investigation do probably contain many "high frequency," components, i.e. wavelengths that are short compared to

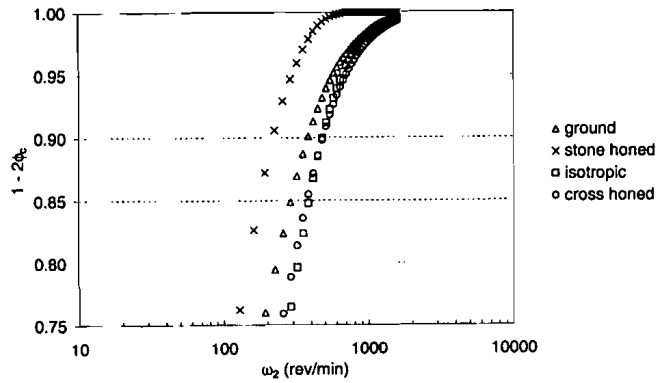

Fig. 11—Theoretical lift-off curve for the processed surfaces. Surface roughness parameters can be found in Table 2.

the contact size, and according to the model, consequently the calculated deformation of the micro-geometry will be very small. Thus the obtained result is close to the one that would be obtained if the deformation of the surface micro-geometry was not accounted for. Hence, for the cases presented here, the roughness wavelength is playing a minor rôle in the ranking of the lift-off speed. This puts in perspective the importance of micro-geometry deformation. The importance of the deformation of the micro-geometry is component dependent and the next step could be to continue the study with processed surfaces with the dominating roughness components in the range where a significant deformation will occur.

CONCLUSION

For an EHL contact with a given micro-geometry on the surface the lubricant film build-up capability was characterised by the so-called "lift-off speed," the speed at which the probability of metallic contact across the gap reaches some small value, assigned in the present work as 5%. The probability of contact is found from a modified Abbott-Firestone curve, in which the in-contact deformation of the micro-geometry has been included and the film gap has been obtained from a nominal smooth film thickness formula. This in-contact deformation can be quite substantial when the wavelength of the micro-geometry is relatively long, and in that case the ranking in lift-off speed found will deviate from the simple R_q ranking.

The objective of the present work has been to validate the predictions of the model by carrying out two-disk experiments on various surfaces. Reiterating that the model by definition is only suited for cases where the amount of asperity contact is small, i.e. the full film side of the lift-off curve, this validation has been quite promising. However, several issues still need to be addressed in future research, e.g. the effect of treating the different frequencies in isolation.

The developed model can be incorporated in easy-to-use engineering software to facilitate analysis of the measured undeformed geometry and the computed deformed surface.

ACKNOWLEDGMENT

The authors would like to thank Dr. M.-L. Dumont and Mr. B.Wemekamp for their work on the development and application of the model, and Mr. R. Vos for his experimental assistance. They would also like to acknowledge Dr. H. Wittmeyer, Research Director, SKF Engineering & Research Centre, for his kind permission to publish this work.

REFERENCES

(1) Ai, X. and Cheng, H. S., (1994), "The Influence of a Moving Dent on Point EHL Contacts," *Trib. Trans.*, **37**, pp 323-335.

(2) Ai, X. and Cheng, H. S., (1994), "A Transient EHL Analysis for Line Contacts, with a Measured Surface Roughness using Multigrid Technique," *ASME Jour. of Trib.*, **116**, pp 549-558.

(3) Ai, X. and Cheng, H. S., (1996), "The Effects of Surface Texture on EHL Point Contacts," *ASME Jour. of Trib.*, **118**, pp 59-66.

(4) Cann, P. M., Ioannides, E., Jacobson, B. and Lubrecht, A. A., (1994), "The Lambda Ratio - a Critical Examination," *Wear*, **175**, pp 177-188.

(5) Cann, P. M., Spikes, H. A. and Hutchinson, J., (1996), "The Development of a Spacer Layer Imaging Method for Mapping Elastohydrodynamic Contacts," *Trib. Trans.*, **39**, pp 915-921.

(6) Chang, L., Cusano, C. and Conry, T. F., (1989), "Effects of Lubrication Rheology and Kinematic Conditions on Micro-Elastohydrodynamic Lubrication," *ASME Jour. of Trib.*, **111**, pp 344-351.

(7) Chang, L. and Webster, M. N., (1991), "A Study of Elastohydrodynamic Lubrication of Rough Surfaces," *ASME Jour. of Trib.*, **113**, pp 110-115.

(8) Christensen, H., (1970), "Stochastic Models for Hydrodynamic Lubrication of Rough Surfaces," in *Proc. Inst. Mech. Engrs.*, **184**, 1, pp 1013-1026.

(9) Dowson, D. and Higginson, G. R., (1966), *Elasto-Hydrodynamic Lubrication, the Fundamentals of Roller Gear Lubrication*, Pergamon Press, Oxford, Great Britain.

(10) Elrod, H. G., (1979), "A General Theory for Laminar Lubrication With Reynolds Roughness," *ASME Jour. of Trib.*, **101**, pp 8-14.

(11) Goglia, P. R., Conry, T. F. and Cusano, C., (1984), "The Effects of Surface Irregularities on the Elastohydrodynamic Lubrication of Sliding Line Contacts. Part I - Single Irregularities," *ASME Jour. of Trib.*, **106**, pp 104-112.

(12) Goglia, P. R., Cusano, C. and Conry, T. F., (1984), "The Effects of Surface Irregularities on the Elastohydrodynamic Lubrication of Sliding Line Contacts. Part II - Wavy Surfaces," *ASME Jour. of Trib.*, **106**, pp 113-119.

(13) Guangteng, G., Cann, P. M., Olver, A. V. and Spikes, H. A., (2000), "Lubricant Film Thickness in Rough Surface, Mixed Elastohydrodynamic Contact," *ASME Jour. of Trib.*, **122**, pp 65-76.

(14) Hamrock, B. J. and Dowson, D., (1977), "Isothermal Elastohydrodynamic Lubrication of Point Contacts, Part III - Fully Flooded Results," *ASME Jour. of Trib.*, **99**, pp 364-376.

(15) Heemskerk, R. S., Vermeiren, K. N. and Dolfsma, H., (1982), "Measurement of Lubrication Condition in Rolling Element Bearings," *ASLE Trans.*, *24*, pp 519-527.

(16) Hooke, C. J., (1997), "Surface Roughness Modification in Elastohydrodynamic Line Contacts Operating in the Elastic Piezoviscous Regime," in *Proc. Inst. Mech. Engrs., Part J., Jour. of Eng. Trib.*, **212 J2**, pp 145-162.

(17) Hooke, C. J., (1999), "Surface Roughness Modification in EHL Line Contacts-the Effects of Roughness Wavelength, Orientation and Operating Condition," in *Proc. 26th Leeds-Lyon Symp. on Tribology, Leeds, 1999*, Elsevier Tribology Series, **36**, Dowson, D. et al., eds., pp 193-202.

(18) Hooke, C. J. and Venner, C. H., (2000), "Surface Roughness Attenuation in Line and Point Contacts," in *Proc. Inst. Mech. Engrs., Part J., Jour. of Engineering Tribology*, **214 J5**, pp 439-444.

(19) Hu, Yuan-Zhong, and Zhu, Dong, (2000), "A Full Numerical Solution to the Mixed Lubrication in Point Contacts," *ASME Jour. of Trib.*, **122**, pp 1-9.

(20) Kaneta, M. and Cameron, A., (1980), "Effects of Asperities in Elasto-hydrodynamic Lubrication," *ASME Jour. of Trib.*, **102**, pp 374-379.

(21) Kaneta, M., Sakai, T. and Nishikawa, H., (1992), "Optical Interferometric Observations of the Effects of a Bump on Point Contact EHL," *ASME Jour. of Trib.*, **114**, pp 779-784.

(22) Kweh, C. C., Evans, H. P. and Snidle, R. W., (1989), "Micro-Elasto-hydrodynamic Lubrication of an Elliptical Contact With Transverse and Three-Dimensional Sinusoidal Roughness," *ASME Jour. of Trib.*, **111**, pp 577-583.

(23) Lubrecht, A. A., ten Napel, W. E. and Bosma, R., (1988), "The Influence of Longitudinal and Transverse Roughness on the Elastohydrodynamic Lubrication of Circular Contacts," *ASME Jour. of Trib.*, **110**, pp 421-426.

(24) Nijenbanning, G., Venner, C. H. and Moes, H., (1994), "Film Thickness in Elastohydrodynamically Lubricated Elliptic Contacts," *Wear*, **176**, pp 217-229.

(25) Patir, N. and Cheng, H. S., (1978), "An Average Flow Model for Determining Effects of Three-Dimensional Roughness on Partial Hydrodynamic Lubrication," *ASME Jour. of Trib.*, **100**, pp 12-17.

(26) Patir, N. and Cheng, H. S., (1979), "Effect of Surface Roughness Orientation on the Central Film Thickness in EHD Contacts," in *Proc. 5th Leeds-Lyon Symp. on Tribology, Leeds, 1978*, Dowson, D. et al. eds., pp 15-21.

(27) Redlich, A. C., Bartel, D., Schorr, H. and Deters, L., (2000), "A Deterministic Model for Point Contacts in Mixed Lubrication Regime," in *Proc. 26th Leeds-Lyon Symp. on Tribology, Leeds, 1999*, Elsevier Tribology Series, **38**, Dowson, D., et al., eds., pp 85-93.

(28) Tripp, J. H., (1983), "Surface Roughness Effects in Hydrodynamic Lubrication: The Flow Factor Method," *ASME Jour. of Trib.*, **105**, pp 458-465.

(29) Venner, C. H., (1991), "Multilevel Solution of the EHL Line and Point Contact Problems," PhD Thesis, University of Twente, The Netherlands, **ISBN 90-9003974-0.**

(30) Venner, C. H. and ten Napel, W. E., (1992), "Surface Roughness Effects in an EHL Line Contact," *ASME Jour. of Trib.*, **114**, pp 616-622.

(31) Venner, C. H. and Lubrecht, A. A., (2000), "MultiLevel Methods in Lubrication," Elsevier Tribology Series, **37**, Dowson, D. et al. eds., **ISBN 0-444-50503-2.**

(32) Venner, C. H., Lubrecht, A. A., and ten Napel, W. E., (1991), "Numerical Simulation of the Overrolling of a Surface Feature in an EHL Line Contact," *ASME Jour. of Trib.*, **113**, pp 777-783.

(33) Venner, C. H. and Lubrecht, A. A., (1994), "Numerical Simulation of a Transverse Ridge in a Circular EHL contact under Rolling/Sliding," *ASME Jour. of Trib.*, **116**, pp 751-761.

(34) Venner, C. H. and Lubrecht, A. A., (1996), "Numerical Analysis of the Influence of Waviness on the Film Thickness of a Circular EHL Contact," *ASME Jour. of Trib.*, **118**, pp 153-161.

(35) Venner, C. H., Couhier, F., Lubrecht, A. A. and Greenwood, J. A., (1997), "Amplitude Reduction of Waviness in Transient EHL Line Contacts," in *Proc. 23rd Leeds-Lyon Symp. on Tribology, Leeds, 1996*, Elsevier Tribology Series, **32**, Dowson, D. et al. eds., pp 103-112.

(36) Venner, C. H. and Lubrecht, A. A., (1999), "Amplitude Reduction of Anisotropic Harmonic Surface Patterns in EHL Circular Contacts under Pure Rolling," in *Proc. 25th Leeds-Lyon Symp. on Tribology, Lyon, 1998*, Elsevier Tribology Series, **36**, Dowson, D. et al. eds., pp 151-162.

(37) Venner, C. H., Kaneta, M. and Lubrecht, A. A., (2000), "Surface Roughness in Elastohydrodynamically Lubricated Contacts," in *Proc. 26th Leeds-Lyon Symp. on Tribology, Leeds, 1999*, Elsevier Tribology Series, **38**, Dowson, D. et al. eds., pp 25-36.

(38) Wedeven, L. and Cusano, C., (1979), "Elastohydrodynamic Film Thickness Measurements of Artificially Produced Surface Dents and Grooves," *ASLE Trans.*, **22**, pp 369-381.

(39) Xu, G. and Sadeghi, F., (1996), "Thermal EHL Analysis of Circular Contacts with Measured Surface Roughnes," *ASME Jour. of Trib.*, **118**, pp 473-483.